Materials Science Forum
ISSN: 1662-9752, Vol. 1197, pp 39-45
doi:10.4028/p-DZQG8k

Submitted: 2026-04-02
Revised: 2026-05-22
Accepted: 2026-05-22
Online: 2026-07-31

Magneto-Mechanical Damping and Phase Transformations in Iron-Based Alloys

Iva Tkalcec[1,a*], Daniele Mari[1,b], Massil Kabchou[2,c] and Igor S. Golovin[3,d]

[1]EPFL, Institute of Physics, CH-1015 Lausanne, Switzerland

[2]Polyech Clermont-Ferrand, 63178 Aubière, France

[3]National University of Science and Technology “MISIS”, 119049 Moscow, Russia

[a]iva.tkalcec@epfl.ch, [b]daniele.mari@epfl.ch, [c]m.mkabchou@gmail.com, [d]i.golovin@misis.ru

Keywords: mechanical spectroscopy, internal friction, Young’s modulus, pure iron, high carbon steel.

Abstract. Internal friction and Young’s modulus were measured for pure iron and a high carbon steel. Temperature dependent measurements in pure iron show a strain dependent component to internal friction below the Curie temperature. It can be attributed to the magneto-mechanical damping as confirmed by amplitude dependent measurements at room temperature with and without magnetic field. The bcc to fcc phase transition on further heating is clearly marked by internal friction peaks in both iron and steel. The effects of cementite dissolution and precipitation in steel are visible on thermal cycling at even higher temperatures.

Introduction

Mechanical spectroscopy is a well-known technique that allows the measurement of the mobility of crystal defects. The defect movement under the stress applied in the elastic range of loading produces damping of sample vibration i.e. energy dissipation during a periodic excitation cycle. Defects of magnetic structure, e.g. magnetic domain walls, especially in ferromagnetic materials, are known to cause damping as well. Such damping is strongly amplitude dependent [1]. Experiments in high purity iron have shown that the magneto-mechanical damping exhibits a maximum that shifts to higher strain amplitudes with the increase of dislocation density [2]. In this paper, we present the results of amplitude dependent damping in pure iron measured at room temperature, as well as temperature dependent internal friction measurements in the high temperature range, which encompasses both the Curie temperature and the bcc ($\alpha -$ phase) to fcc ($\gamma -$ phase) transition. A sharp peak corresponding to the bcc-fcc transition was also found e.g. in some Fe-Ga alloys, more specifically A2($D0_3$) bcc to $L1_2$ fcc [3],[4]. The temperature dependent measurements in iron are compared with those of a high carbon tool steel where magnetic and phase transitions occur simultaneously.

Experimental

Two materials were studied. The first is a pure iron containing less than 0.02% of other elements. The second is a high carbon tool steel containing 1.23 wt.% carbon and 0.64 wt.% chromium that is mostly retained in cementite (hypereutectoid) spheroidal precipitates. Cementite carbides spheroidized in the primary thermal treatment at 1150 K range from 0.2 to 2 μm in diameter and occupy 12 ± 2 % of the volume. As confirmed in [5], the actual composition of the iron matrix is just below the eutectic with a maximum of 0.4 wt.% C obtained by quenching from 1100 K.

Amplitude Dependent Internal Friction (ADIF) measurements are made in a free pendulum capable to produce high strain amplitude oscillations up to a maximum strain of $2.2 \cdot 10^{-3}$ at a resonant frequency of about 2 Hz. A magnetic field of 0.056 T could be applied axially around the sample to saturate magnetisation. Temperature scans are realized in a forced pendulum at strain amplitudes of $1 \cdot 10^{-5}$ and $1 \cdot 10^{-4}$ and at frequencies of 0.2 and 1 Hz. Heating and cooling rate was 2 K/min.

Results

The spectra measured in pure iron as a function of temperature on heating and cooling are shown in Fig. 1a. Two maxima in internal friction are found: at about 760 K and at 920 K. The maximum found at 920 K has an amplitude much higher in cooling than in heating when the strain amplitude is $1 \cdot 10^{-4}$. Moreover, the shape of the maximum is also different. Another observed feature is a dip in internal friction and modulus between 1020 and 1040 K, which is expected to be the transition from the ferromagnetic to the paramagnetic state of sample close to the Curie temperature. If the strain amplitude is decreased from 10^{-4} to 10^{-5}, the whole spectrum shows a lower level of internal friction, but particularly the maximum present at 920 K at 10^{-4} is hardly visible at 10^{-5} and there is almost no difference between heating and cooling.

Fig. 1b shows the temperature spectra measured for two different frequencies at the strain amplitude of $1 \cdot 10^{-4}$ on heating and cooling. If the frequency is changed from 1 Hz to 0.2 Hz, both peaks and the high temperature background slightly shift to lower temperatures. However, the onset of the IF increase and modulus plateau are not affected.

The ADIF measurements performed on the same sample at room temperature are presented in Fig. 2. In case of no additional magnetic field, there is a strong amplitude dependent internal friction with a maximum for strain amplitude about $5 \cdot 10^{-4}$. If an axial saturation magnetic field is applied, this maximum completely disappears, there is only a smaller internal friction increase at high amplitudes, present also with no field. The difference curve (obtained using interpolated values as the measured points do not have exactly the same strain values) is also plotted showing a maximum of magneto-mechanical damping (Fig. 2a). After removing the magnetic field, the first measurement displays a transient effect, the internal friction remains lower until a maximal strain amplitude is reached, after which the maximum is again seen at the initial level (Fig. 2b).

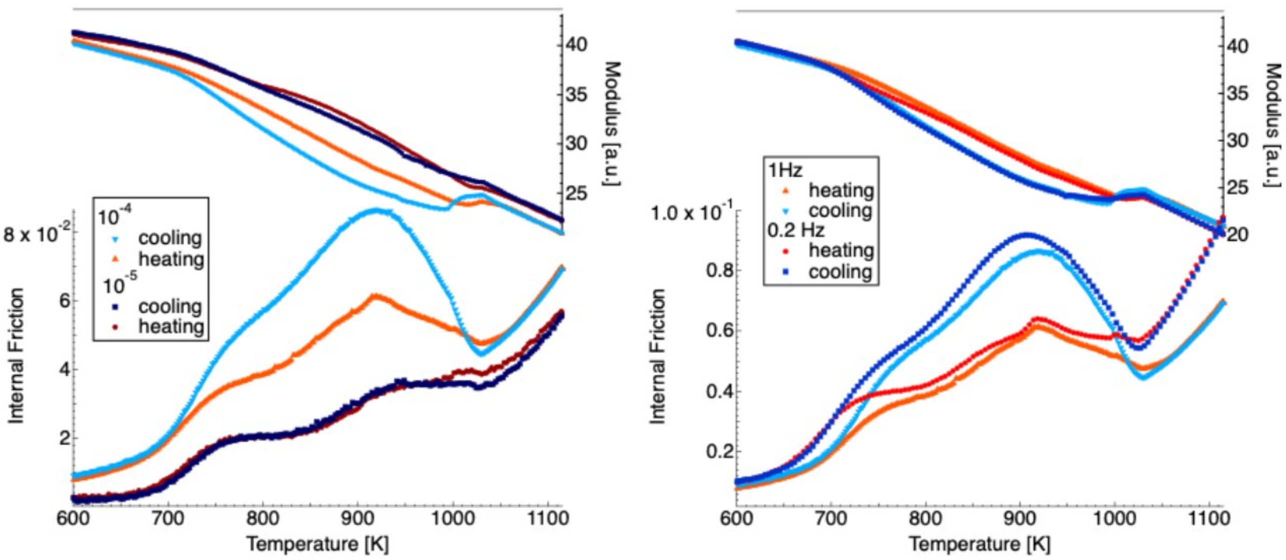

a) b)

Fig. 1. Internal friction and shear modulus in pure iron measured as a function of temperature at two different strain amplitudes at 1Hz (a) and at two different frequencies at a strain of $1 \cdot 10^{-4}$ (b).

Fig 3a. presents temperature dependent internal friction and shear modulus in pure iron measured at higher temperatures, where the α to γ phase transition is expected on heating. An IF peak and a modulus dip are observed at 1180 K on heating, and an IF peak and modulus decrease appear at 1170 K on cooling.

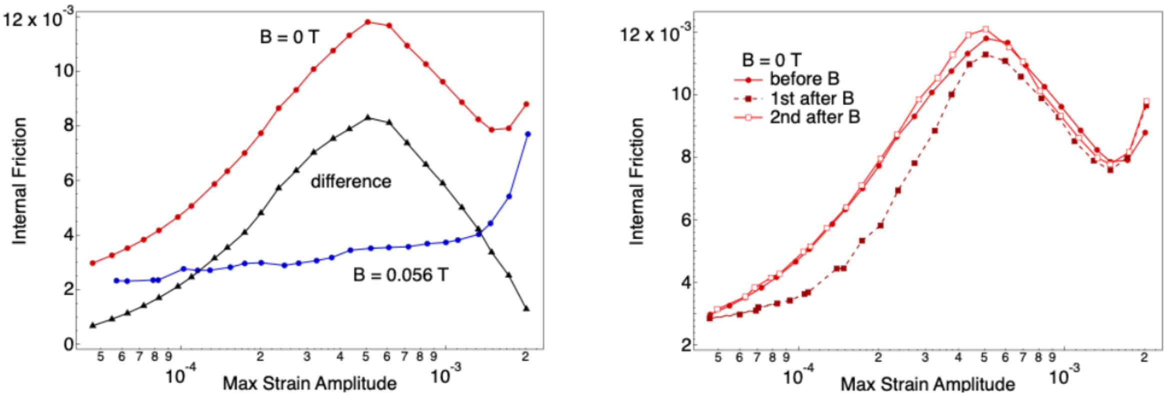

a) b)

Fig. 2. Amplitude dependent internal friction in pure iron. a) Measurements with and without axial magnetic field of 0.056 T at about 2 Hz and their difference. b) Comparison of measurements without external magnetic field, before and after it was applied.

The same measurements made on high carbon tool steel are presented in Fig. 3b accompanied by a calorimetry measurement (DTA at 5 K/min). The measurements presented in Fig. 3 are reproducible on heating up to the maximal temperature presented and on the following cooling both for iron and steel samples.

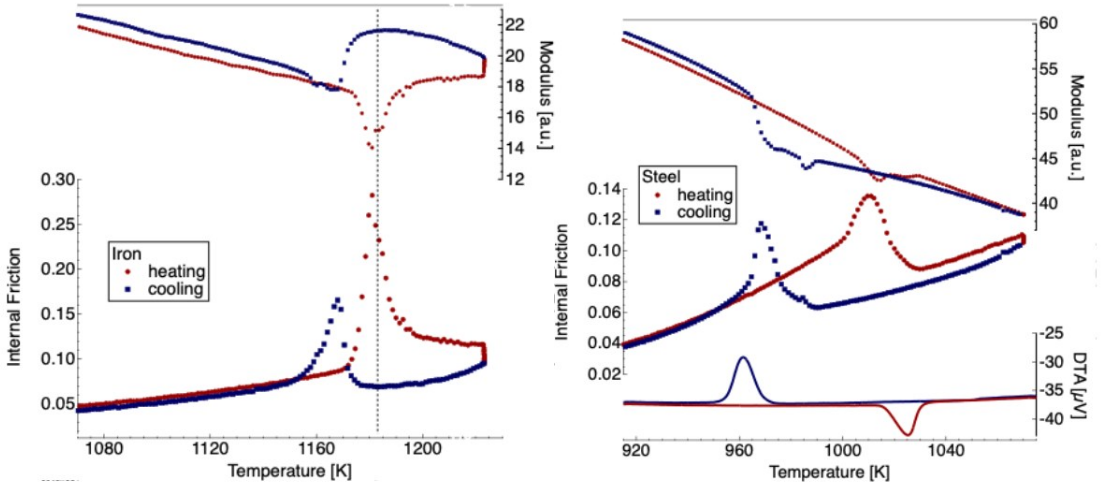

a) b)

Fig. 3. Internal friction and shear modulus as a function of temperature measured at 2 K/min and 1Hz in pure iron at strain amplitude of $1\cdot10^{-5}$ (a) and in high carbon steel measured at strain amplitude of $5\cdot10^{-5}$ (b). A dotted line in a) marks the temperature of 1183 K corresponding to the bcc-fcc transition in pure iron. Calorimetry measurements (DTA) at 5 K/min in high carbon steel are added for comparison in b).

Fig. 4 presents the measurements in the high carbon steel on high temperature thermal cycling. On heating, the internal friction is much higher, and the modulus lower when measured after the sample was quenched from 1100 K (heating 1). An abrupt IF decrease is observed on heating starting at 1000 K and another more gradual one starting at 1150 K, both accompanied by a modulus increase. On cooling, a smaller IF maximum is visible at about 1120 K accompanied by a strong modulus increase. If the cooling is condinued (cooling 2), an abrupt and much stronger IF increase can be observed starting at 995 K, accompanied by a small dip in the modulus. However, if the cooling is stopped at 1040 K, the internal friction is even somewhat lower in the following heating (heating 2), and a maximum is observed at 1225 K. The corresponding modulus remains high in heating until a drop, starting around 1200 K.

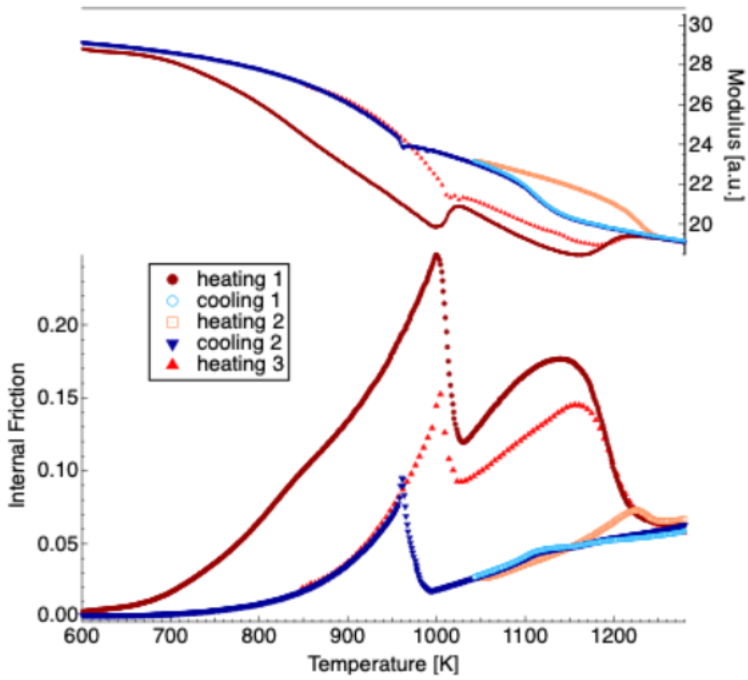

Fig. 4. Internal friction and modulus in high carbon steel measured on high temperature thermal cycling starting with first heating after the sample was quenched from 1100 K.

Discussion

The peak observed around 760 K in pure iron is analogue to those found in [6], [7], [8] and the authors attribute it to grain boundary sliding. Its height does not depend on the strain amplitude (Fig. 1a) and the peak is clearly thermally activated (Fig. 1b). Since such phenomenon is not the focus of this paper it will not be discussed any further.

The internal friction peak observed around 920 K is most likely related to magnetic damping in the ferromagnetic phase as the internal friction increase in cooling starts abruptly below 1040 K, which coincides with the Curie temperature. It shows a clear amplitude dependence (especially in cooling, (Fig. 1a)) and it is frequency independent. The modulus plateau or anomaly found below the Curie temperature correlates well with the lattice parameter plateau observed by [9]. Unfortunately, for technical reasons, it was not possible to perform measurements at such high temperature under an external magnetic field, which would have irrefutably proven the magnetic origin of the peak. Such measurement was possible only at room temperature (Fig. 2) and for a fixed frequency (free decay pendulum). The magneto-mechanical damping, calculated as the difference between the internal friction measured without the external magnetic field and the one measured under a magnetic field (Fig. 2a), shows a clear maximum. Such behaviour is expected for ferromagnetic materials and is explained by the stress-induced movement of magnetic domain walls [10]. A behaviour very similar to that exposed in Fig. 2 was found by one of the authors in Fe-Cr alloys and in pure iron [1]. In previous measurements made on high-purity iron [1], [2] at room temperature, the maximum was situated at strain amplitudes in the range $(2\text{-}5)\cdot 10^{-4}$ depending on the annealing temperature after cold work in ref. [1]. In ref. [2], where cold-work strains up to 3% were applied at RT and at liquid nitrogen temperature, the maximum was located below $1\cdot 10^{-4}$ In the present experiment the value of $4\cdot 10^{-4}$ indicates the presence of high internal stresses or high dislocation density [2]. The applied axial magnetic field of 0.056 T is high enough to completely suppress the magnetic contribution, but after it is removed, a relatively high strain amplitude is needed to replicate a distribution of magnetic domain walls that produces the initial peak height (Fig. 2b).

When the temperature dependent measurements are made in pure iron above Curie temperature, where magnetic damping is completely absent, a clear signature of the ferrite-austenite phase transition expected at 1183 K is observed both in internal friction and the modulus measurements (Fig. 3a). An internal friction peak and a corresponding dip in the modulus accompany the phase transition in both heating and cooling with a hysteretic behaviour expected for first order phase transitions. To the best of our knowledge this is the first measurement by mechanical spectroscopy of the bcc-fcc transformation in pure iron.

The mechanical spectroscopy measurements in steel also show maxima corresponding to the phase transitions in the material, but the characteristic signatures are modified by the presence of carbon. According to the equilibrium phase diagram, the ferrite to austenite (bcc to fcc) phase transition is expected to occur at ~ 996 K and therefore coincides with the ferromagnetic to paramagnetic transition. Additionally, as the carbon solubility differs strongly in bcc and fcc structure, the transition is accompanied by the dissolution of cementite in heating and precipitation on cooling. Similar to what was observed in iron, the phase transition in steel is marked with peaks in internal friction (Fig. 3b), which start to appear at 1000 K and 995 K in heating and cooling respectively. This transition is also clearly marked in calorimetry measurements, although with a somewhat larger hysteresis due to the faster heating and cooling rate: 5 K/min in calorimetry, with respect to 2 K/min for mechanical spectroscopy. The difference in the temperatures observed in the IF and calorimetry measurements might be due to the high sensitivity of mechanical spectroscopy to defect movement that might cause precursor phenomena to the actual transformation. Such difference between calorimetry and IF was found in martensitic transformation studies [11]. When compared to pure iron, a notable difference is observed in the modulus behaviour of steel on cooling. In pure iron, the fcc to bcc transformation is marked by a modulus decrease, while the opposite is seen in steel where the modulus increases. This increase can be attributed to the increase of the elastic modulus due to the precipitation of carbon, which was in solid solution in the fcc phase [12].

Due to the strong temperature (phase) dependence of carbon solubility in steel, the mechanical spectroscopy spectra strongly depend on the thermal history of the sample (Fig. 4). The internal friction is much higher, and the corresponding modulus lower, in first heating after quenching with respect to the following cycles when the sample is heated following a very slow cooling. If the sample is quenched from 1100 K, the resulting microstructure is martensitic that is characterized by a very high dislocation density. The first heating is expected to produce very small cementite carbide particles decorating the dislocations distributed in the matrix [13]. On the other hand, slow cooling is more likely to produce a pearlitic microstructure where large cementite lamellae are intertwined with the ferrite. These cementite lamellae, as well as the large spheroidal cementite particles are expected to remain stable below 1150 K. When the sample is heated to the maximal temperature of 1300 K, a full carbon solubility is expected, and even the large carbide particles are expected to start dissolving. Moreover, a relatively low internal friction is expected for a well annealed austenitic structure. Therefore, the decrease of internal friction observed between 1150 and 1200 K should be attributed to the cementite solution and dislocation restoration. However, the dissolution process is likely to be very slow and there are no visible peaks associated to these microstructural changes in calorimetry measurements. On cooling from 1300 K (Fig. 4, cooling 1 and 2), there is a small internal friction maximum at around 1100 K, and the modulus increases as the concentration of dissolved carbon decreases below 1150 K. Instead, the variation of the modulus on heating is strongly dependent on thermal history. If the cooling ramp is stopped above 1000 K (cooling 1, Fig. 4) in the austenitic phase, the internal friction shows a small peak at 1050 K. In the following heating (heating 2), the modulus remains high and the internal friction low. Then, at around 1150 K, the modulus decreases again. As observed in [14], the Young's modulus is expected to decrease as the carbon concentration increases. We expect the modulus variations to be related to the change of the amount of dissolved carbon in austenite that affects the purely elastic Young's modulus. The hysteretic behavior of the elastic modulus between 1100 K and 1200 K is also in agreement with phase diagrams of similar high carbon chromium steels such as SAE 52100, where the transition between homogeneous austenite and austenite-cementite phases is expected at around 1150 K for 1%C [15], [16], [17]. Clearly, the precipitation and dissolution of the secondary cementite can occur with a certain delay with respect to equilibrium. If the sample is cooled below 1000 K (cooling 2), austenite transforms to pearlite and the dislocation density also increases in the ferrite. On following heating (heating 3), the internal friction clearly shows the bcc-fcc transformation peak although not as high as in quenched sample. At 1150 K, upon cementite dissolution, the internal friction strongly decreases and modulus increases. The internal friction decrease can be related to the decrease of the dislocation density. Such a strong decrease of the internal friction is accompanied by the increase of the dynamic modulus as already observed on the first heating.

Conclusion

Both magnetic and structural phase transitions were observed by mechanical spectroscopy in pure iron. It can be inferred that the onset of the paramagnetic to ferromagnetic transition in cooling can be detected by mechanical spectroscopy via a sudden increase of damping. A dip, corresponding to the Curie temperature, is also detected in the modulus. These effects are much more pronounced for high strain amplitude that enhances the magneto-mechanical contribution. In heating, the effect is much lower, but still clearly marked. This means that the rearrangement of domain walls out of equilibrium when temperature is decreased leads to a higher magneto-mechanical damping. Instead, upon heating the magnetic structure is frozen and the magneto-mechanical damping lower. A strong ADIF is observed in pure iron at room temperature. This effect is suppressed under axial magnetic field indicating its magnetic origin. By comparing the temperature spectra of pure iron and steel we can detect a clear signature of ferrite to austenite phase transitions in both materials as a sharp internal friction peak. However, in steel, the transformation occurs in the same temperature region as that of the ferromagnetic to paramagnetic transformation. Instead, in iron, only microstructure effect can be attributed to the transformation peak that occurs at 1180 K on heating. The solid solution state of carbon in steel produces some complex effects on both internal friction and the modulus, that are not easy to discriminate without a systematic study that is outside the scope of this paper.

References

[1] I.S. Golovin, Mechanism of Damping Capacity of High-Chromium Steels and α-Fe and Its Dependence on Some External Factors, Metall. Mater. Trans. A. 25 (1994) 111–124.

[2] J. Degauque, B. Astie, L. P. Kubin, Evidence for the interaction between magnetic domain walls and dislocations in high-purity iron from magnetomechanical damping experiments, physica status solidi (a) 45.2 (1978): 493-501.

[3] I.S. Golovin, V.V. Palacheva, A.I. Bazlov, J. Cifre, N. Nollmann, S. V Divinski, G. Wilde, Diffusionless nature of $D0_3$ / $L1_2$ transition in Fe_3Ga alloys, J. Alloys Compd. 656 (2016) 897–902.

[4] I.S. Golovin, V.V. Palacheva, A.I. Bazlov, J. Cifre, J. Pons, Structure and anelasticity of Fe_3Ga and Fe_3(Ga, Al) type alloys, J. Alloys Compd. 644 (2015) 959–967.

[5] I. Tkalcec, D. Mari, W. Benoit, Correlation between internal friction background and the concentration of carbon in solid solution in a martensitic steel, Mater. Sci. Eng. A. 442 (2006) 471–475.

[6] G.M. Leak, Grain Boundary Damping I: Pure Iron, Proc. Phys. Soc. 78 (1961) 1520–1528.

[7] P. Barrand, Grain boundary relaxations in iron-chromium alloys, Acta Metall. 14 (1966) 1247–1256.

[8] M. Sun, W. Jiang, X. Liu, T. Chen, X. Wang, Q. Fang, A comparative study on the grain boundary internal friction peak of pure iron, Materials Letters 305 (2021) 130814.

[9] N. Ridley, H. Stuart, Lattice parameter anomalies at the Curie point of pure iron, Journal of Physics D: Applied Physics 1.10 (1968) 1291.

[10] G.W. Smith, J.R. Birchak, Internal stress distribution theory of magnetomechanical hysteresis- an extension to include effects of magnetic field and applied stress, Journal of Applied Physics 40.13 (1969) 5174-5178.

[11] D. Mari, L. Bataillard, D.C. Dunand, R. Gotthardt, Martensitic Transformation of NiTi and NiTi-TiC Composites, 5 (1995) 659–664.

[12] G. R. Speich, W. C. Leslie, Elastic constants of martensite, Metallurgical Transactions 4 (8) (1973) 1873-1875.

[13] I. Tkalcec, C. Azcoıtia, S. Crevoiserat, D. Mari, Tempering effects on a martensitic high carbon steel, Materials Science and Engineering: A 387 (2004) 352-356.

[14] W. J. Arnoult, R. B. McLellan, Variation of the Young's Modulus of Austenite with carbon concentration, Acta Metallurgica 23.1 (1975) 51-56.

[15] J. Epp, H. Surm, O. Kessler, T. Hirsch, In situ X-ray phase analysis and computer simulation of carbide dissolution of ball bearing steel at different austenitizing temperatures, Acta Mater. 55 (2007) 5959–5967.

[16] D. Foster, M. Paladugu, J. Hughes, M. Kapousidou, U. Islam, A. Stark, N. Schell, E. Jimenez-Melero, In-situ synchrotron X-ray diffraction during quenching and tempering of SAE 52100 steel, Mater. Today Commun. 29 (2021) 102930.

[17] H. Hwang, B.C. De Cooman, Influence of the Initial Microstructure on the Spheroidization of SAE 52100 Bearing Steel, Steel Res. Int. 87 (2016) 112–125.

The publication of this article was funded by the Swiss Federal Institute of Technology in Lausanne 10.13039/501100001703